

(NASA-CR-196111)  
MICRO-MEASUREMENTS OF MECHANICAL  
PROPERTIES FOR ADHESIVES AND  
COMPOSITES USING DIGITAL IMAGING  
TECHNOLOGY Final Report (Texas  
Univ.) 18 p

N95-10231

Unclass

G3/24 0014046

11-24-94  
14-16  
18P

**Final Report**  
**UTSA - MM<sup>2</sup> Lab Report No. 6274, June 27, 1994**

**Micro-Measurements of Mechanical Properties  
for  
Adhesives and Composites Using Digital Imaging  
Technology**

**Hal F. Brinson, Professor**  
**Division of Engineering**  
**University of Texas at San Antonio,**  
**San Antonio, TX 78249-0601**  
**Ph: 1-210-691-5511**  
**FAX: 1-210-691-5589**  
**E-Mail: hbrinson@lonestar.utsa.edu**  
**or**  
**hal brinson @aol.com**

**Submitted as a final report\* for:**

- NASA Ames Research Cooperative Agreement, NCC 2-724.
- ONR Contract, N00014-82-K-0185 through Virginia Tech (CR-4303-430220).

**Submitted as an interim report\* for:**

- Boeing Commercial Airplane Company contract, Boeing - T2 - 341085 / 8BO3.

**Prepared for:**

- Presentation at the 10th International Conference on Experimental Mechanics, Lisboa, Portugal, July 18-22, 1994 and to be published in the conference proceedings.

- \* This report details activity performed at UTSA in the micro-measurement/micro-mechanics laboratory. An additional report for activities performed at NASA Ames was submitted earlier by Dr. Clement Hiel (see report dated October 6, 1993). Most of the equipment used herein was purchased with ONR funds while most of the student support was funded by NASA and Boeing.

# Digital imaging micro-measurements of properties for adhesives and composites

Hal F. Brinson, Professor  
University of Texas at San Antonio, San Antonio, TX 78249-0601

**ABSTRACT:** The need for a constituent based durability or accelerated life prediction procedure to be used for the engineering design of polymer matrix composites is discussed in the light of current plans for the High Speed Civil Transport (HSCT), concerns about the U. S. infrastructure (bridges, pipelines, etc.) and other technological considerations of national concern. It is pointed out that good measurement procedures for insitu resin properties are needed for both adhesives and composites. A double cantilever beam (DCB) specimen which shows promise for the easy determination of adhesive shear properties is presented and compared with measurements of strains within the bondline using a new optical digital imaging micro-measurement system (DIMMS). The DCB specimen is also used to assess damage in a bonded joint using a dynamic mechanical thermal analysis system (DMTA). The possible utilization of the same DIMMS and DMTA procedures to determine the insitu properties of the resin in a composite specimen are discussed as well as the use of the procedures to evaluate long term mechanical and physical aging. Finally, a discussion of on the state-of-the art of the measurement of strains in micron and sub-micron domains is given.

## INTRODUCTION

At the 6th International Conference on Experimental Stress Analysis in Munich in 1978 the author presented details of a new procedure for the accelerated life prediction of advanced composite materials [1]. It was noted that a reason that inhibited the use of polymer matrix composite (PMC) materials in many structural applications was uncertainty about their long term response under adverse environmental conditions. While it was noted that fatigue was a factor, it was also noted that the intrinsic viscoelastic nature of the polymer matrix could lead to delayed failures long after composite components were first put into service. Tests which had been conducted by Y. T. Yeow and the author while in residence at NASA-Ames Research Center demonstrated that significant viscoelastic processes occurred at room temperature at high stress levels. Indeed, it was shown that a relaxation to failure phenomena occurred in a uniaxial

tensile test of a matrix dominated [ $\pm 45^\circ$ ] composite laminate [1,2]. For this reason, concern was expressed about the possibility of catastrophic failure in PMC structures if procedures were not developed to understand and predict their occurrence. For this reason, the author introduced for the first time at the 6th Conference a procedure for the accelerated life prediction of PMC materials. The fundamental idea was to use the well known time-temperature-superposition-principle (TTSP) for polymers to determine the long term response of the matrix dominated properties of PMC materials using short term testing procedures. Both changes in modulus and strength were considered. Initial testing and analysis were limited to linear considerations. However, it was soon realized that failure, however defined, is a non-linear process. As a result, modifications were introduced which allowed the development of long term master curves for modulus (and strength) by introducing

stress as an accelerating parameter as well as temperature [3-11].

In the light of possible new applications for composite materials such as the high speed civil transport (HSCT), off-shore structures, bridges, pipelines, etc., the need to insure durability over the life (perhaps as long as 50 years) of a composite structure has become a major technological issue. Obviously testing programs to insure product durability over such time scales would severely inhibit the use of potential new materials. Indeed, it is felt that some possible candidates for the resin of new composites that may be used in the HSCT have not yet been invented. For these reasons, a reliable accelerated life prediction procedure is urgently needed to address such new issues as physical and chemical aging as well as the intrinsic viscoelastic nature of polymer based materials.

For the above reasons it is appropriate to examine again the accelerated life prediction methods discussed at the 6th Conference. The procedure outlined at that time, and subsequently modified, utilized short term creep testing on unidirectional laminates in combination with nonlinear viscoelastic constitutive models of Schapery and Knauss [3,8] and time dependent failure theories of Zurkhoff and Crochet [4,12]. These analytical models were incorporated into incremental laminated plate or finite element approaches that use the experimentally determined lamina constituent master curves for moduli and strengths to predict the response of general laminates with arbitrary fiber directions. Long term test programs as long as three months have been used to verify general laminate predictions [7].

Recently, the necessity to develop engineering design procedures for composites visualized for the HSCT has suggested a reexamination of our approach to consider the feasibility of using knowledge of the time variation of resin and interface properties as the constituents needed in incremental predictive techniques. A possible method would be to test the resin in

neat or bulk form. However, our earlier work suggests that bulk properties of the resin are not necessarily the same as those found in the cured composite. As a result, a new optical digital imaging micro-measurement system (DIMMS) is being developed which may eventually be useful in determining the properties of the resin (and perhaps the interface) by making measurements of strains in resin rich regions between plies or between fibers within a cured composite. The present paper will detail the present DIMMS methods under development and currently being used to determine the properties within the bondline of adhesives and within fiber reinforced composites.

The principle focus of the development of the DIMMS has been the need to have a simple and reliable procedure to determine the pure shear properties of an adhesive and perhaps the interphase by measuring strains within the bondline and/or within the interphase. This is best accomplished by having a specimen geometry such that a pure shear state exists within the bondline. In recent years, a number of specimens have been suggested in which a uniform and pure shear stress state exists in the adhesive layer. These include the Iosipescu and the Arcan geometries [13] and a new end loaded bonded double cantilever beam specimen (label the BMC for simplicity) introduced by the author and his colleagues [13-16]. The latter specimen has appeal as a three point bend test is nothing more than two back-to-back cantilever beams. As a result, a simple and inexpensive approach to measuring pure shear properties is now available for industry. The objective of this paper is to provide an overview of the use of the DIMMS approach for the determination of strains within the bondline of the BMC specimen. It will also be shown that a modified BMC specimen can be used in association with a dynamic mechanical thermal analyzer (DMTA) as a means of assessing damage in a bonded joint. Finally, a discussion of the use of the DIMMS to measure the strains within resin rich regions of a

However, it should be noted that the overall goal is to develop an experimental method in which strains can be measured within micron and sub-micron regions.

### ADHESIVE SHEAR PROPERTIES USING A DOUBLE CANTILEVER BEAM

The bonded cantilever beam loaded at the end as show below in Fig. 1 will bend in such a manner to produce a pure shear stress in the adhesive layer. This is easily

recognized by examining the deformations of the top and bottom adherends and noting that the bottom of the top adherend will deform exactly the same amount as the top of the bottom adherend but in the opposite direction. A detailed examination of the deformed adherends is given in reference [15].

Moussiaux [15] developed a differential equation for the shear stress in the adhesive layer using elementary beam theory into which expressions of moment equilibrium and compatibility of deformations were substituted.

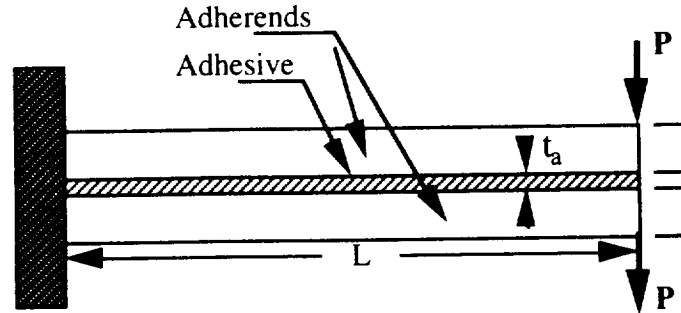


Figure 1. Adhesively bonded cantilever beam.

The differential equation was then solved to obtain the shear stress distribution in the adhesive layer along the length of the bond line and the standard Euler-Bernoulli beam deflection equation was

solved to obtain beam deflections. The resulting equations for adhesive shear stress along the length of the beam and the deflection at the free end were given as:

$$\tau_{xy} = \frac{P}{by^2(h+2t)} [1 - \cosh(\alpha\xi) + \tanh(\alpha)\sinh(\alpha\xi)] \quad (1)$$

$$\delta = \beta P \frac{L^3}{2Eb(h+t)^3} \quad (2)$$

where  $\tau_{xy}$  is the shear stress,  $L$  is the beam length,  $\xi = x/L$  is the non-dimensional distance along the beam,  $b$  is the beam width,  $h$  is the adherend thickness and

$2t = t_a$  is the adhesive thickness. The parameters  $\alpha$ ,  $\beta$  and  $\gamma$  were found to have the following form

$$\alpha = \gamma \sqrt{3 \frac{G_a}{E} \left(\frac{L}{h}\right)^2 \frac{\left(1 + 2 \frac{t}{h}\right)^2}{\frac{t}{h}}} \quad \gamma = \sqrt{1 + \frac{1}{3 \left(1 + 2 \frac{t}{h}\right)^2}}$$

$$\beta = \left(\frac{h+t}{h}\right)^3 \left[ 4 \left(1 - \frac{1}{\gamma^2}\right) + \frac{3E}{G_a} \left(\frac{h}{L}\right)^2 + \frac{12}{\alpha^2 \gamma^2} \left(1 - \frac{1}{\alpha} \tanh \alpha\right) \right]$$

where  $G_a$  is the adhesive shear modulus and  $E$  is the modulus of the adherend. As may be seen,  $\alpha$ ,  $\gamma$  and  $\beta$  are functions of the beam geometry and the moduli of the adhesive and adherends. These parameters were found in reference [15] by forcing continuity at the centerline of the ad-

hesive. Instead, if continuity is enforced at the interface between adherend and adhesive, the following equations for adhesive shear stress along the length of the beam and end deflection are found:

$$\tau_{xy} = \frac{3P}{4bh} [1 - \cosh Ax + \tanh AL \sinh Ax] \quad (3)$$

$$\delta = \beta_b \frac{PL^3}{2Ebh^3} \quad (4)$$

where

$$A = \sqrt{\frac{8}{ht_s} \frac{G_a}{E}} \quad \text{and} \quad \beta_b = \frac{PL^3}{2Ebh^3} \left[ \left(1 + \frac{9t_s hE}{4L^2 G_a}\right) - \frac{9}{8} \frac{t_s hE}{L^2 G_a} \tanh(AL) \sqrt{ht_s \frac{E}{G_a}} \right]$$

In (3) and (4) all terms are as defined previously except  $A$  is a new parameter related to the specimen geometry and to the properties of the adhesive and adherends. (It should be noted that in this development, the adhesive thickness is taken as  $t_a$  rather than  $2t$  as in Moussiaux.) Details of these results can be found in reference [17] and are being published separately. As shown in reference [17], optimum beam dimensions are easier to obtain using equations (3) and (4) rather than equations (1) and (2). In either case, it is possible to optimize the beam dimensions such that the shear stress in the adhesive layer is independent of adhesive and adherend moduli and the shear stress can be made to be constant over a large portion of the beam.

Using the formulation given in equation (3), a symbolic equation solver such as MATHCAD easily gives the stress distribution along the length of the beam. Figure 2 shows the resulting stress distribution for aluminum bonded with both epoxy and polyurethane as obtained for a typical set of dimensions. The shear stress is uniform over a large portion of the beam for an epoxy adhesive but not for a urethane adhesive (using the same dimensions as in the epoxy beam). The latter could be made more uniform with a different set of dimensions. Moussiaux obtained similar results and verified his calculations with a finite element program [15]. Fior, experimentally verified Moussiaux's solution and used a finite

element program to examine a number of different loading cases [16]. She showed little difference resulted if a concentrated load of  $2P$  was used only on top of the beam as opposed to a load of  $P$  on both the top and bottom of the beam as show in Fig. 1. This is important if a three point

bend beam is used rather than a cantilever. The revised solution [17] for shear stresses and deflections given by equations (3) and (4) is shown to be only slightly different from those of Moussiaux [15] and those of Fior[16].

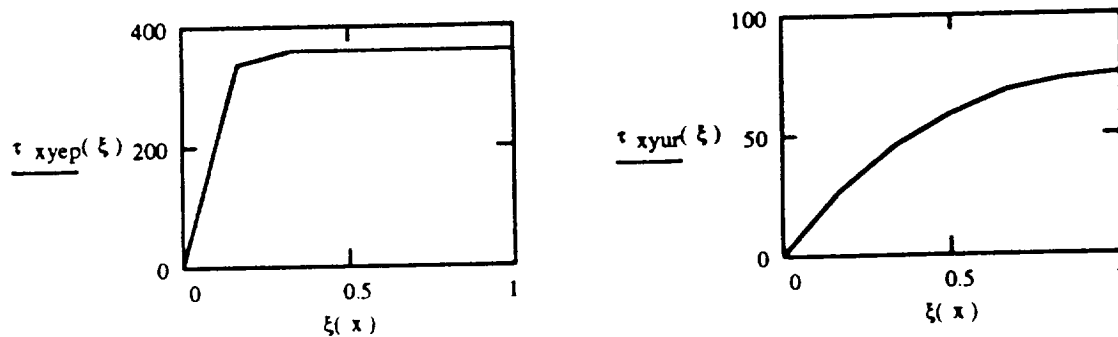


Figure 2. Distribution shear stress along aluminum beam bonded with epoxy (left). or urethane (right) [17].

### Dynamic Mechanical Thermal Analysis (DMTA) Studies of a Fixed/Fixed Beam

Li, Dickie and Morman [18,19] extended Moussiaux's solution to the case of a fixed/fixed viscoelastic beam (Fig. 3) un-

der steady state oscillations using Fourier transforms. The fixed/fixed beam was chosen as it is the required geometry in the DMTA used in their experimental program. The DMTA is designed to give storage and loss moduli and/or damping

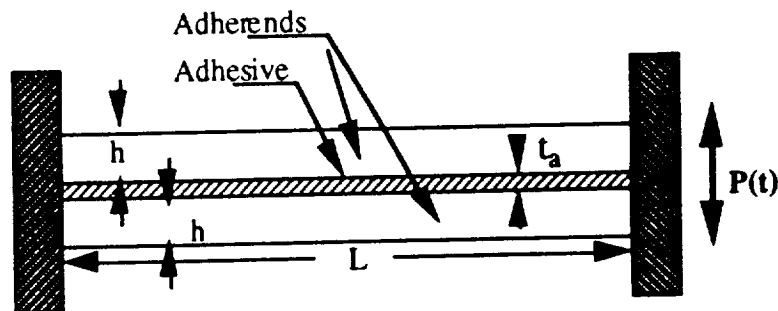


Figure 3. Adhesively bonded fixed/fixed beam in steady state oscillation.

behavior for monolithic polymeric beams and these quantities are indicative of the polymer investigated. However, DMTA output for a bonded beam will be composed of contributions from both the ad-

herend and the adhesive bond and therefore will not give a definitive number for the moduli and damping ratio of only the bonding process. The unique feature of the viscoelastic solution of Li, Dickie and

Morman is that it does provide a method by which unique shear moduli and damping properties of the adhesive can be separated from the flexure properties of the total beam. A detailed description of the procedure is given in reference [19]. It is appropriate to note that the simplification afforded by enforcing continuity at the interface rather than the middle of the adhesive layer will result in simplified procedures to obtain adhesive viscoelastic properties using the DMTA. Such efforts are in progress and will be reported subsequently.

### Digital Imaging Micro-Measurement System (DIMMS)

A schematic of the digital imaging micro-measurement system is shown in Fig. 4. The system includes a miniature screw driven constant head rate testing machine

(Minimat) which is fixed to the stage of an optical microscope. Small tensile, compressive, beam or other type specimens can be loaded as with a conventional large constant head rate testing system. In the study reported herein a special fixture was designed to accommodate beam type specimens loaded in three point bending. Also, a specially designed platform (not shown) allows the stepper motor and flexible drive shaft to move with the micrometer controlled stage of the microscope. Thus, specimens can be located anywhere within the working dimensions of the test frame. The maximum load that can be delivered to the specimen is 1,000 Newtons. The miniature test system includes a thermal chamber with a viewing window and both force and deformation is computer controlled. Deformation is determined from the motion of the screw while force is measured via the motion of an LVDT attached to a calibrated beam within the movable head of the frame.

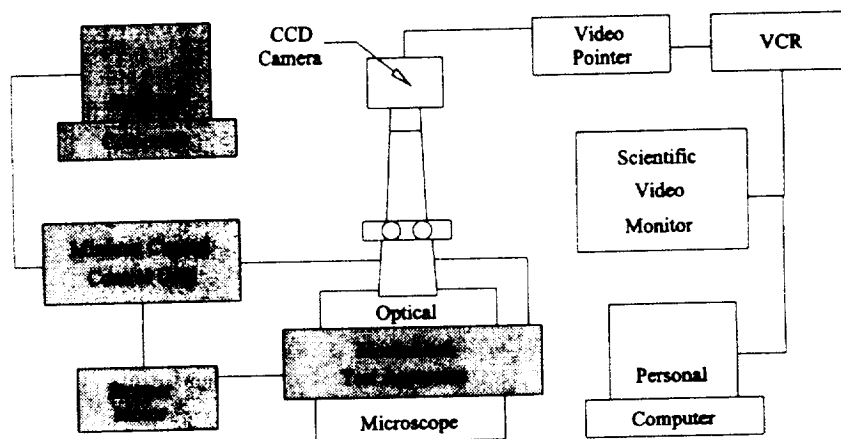


Figure 4. Schematic of digital imaging micro-measurement system.

Magnifications of 1,000 x are possible with the binocular optical microscope. Attached to the microscope is a RS 170 CCD camera with a 768 x 494 pixel map. The CCD camera sends an image of the specimen to a video monitor via a video recorder (VCR) and simultaneously to a computer containing a 512 x 400 pixel frame grabber board. With this system, an

object can be viewed in real time with the microscope binoculars, in real time on the video monitor and can be recorded on the VCR for later viewing.

A computer software package allows the pixel map of the frame grabber board to serve as a means of locating specific points on the object and thereby measuring distances from one point to another.



Obviously, changes in distance between two points can be measured in the same manner and these measurements can be converted into strain. With DIMMS, measurements of distances, displacements or deformations can be made with the micrometer controlled microscope stage as well as the CCD camera and the frame grabber board. Therefore, a built in method is available to verify measurements made with the CCD camera.

To determine the accuracy of the measuring process with the DIMMS system, a precision calibration scale with the smallest division of  $10\text{ }\mu\text{m}$  was viewed with the microscope. The digitized image at  $1,000\times$  magnification is shown in Fig. 5 (top left). The software allows for computer generated image enhancement and/or amplification of the image by as much as eight fold. That is, the  $1,000\times$  image can be doubled to  $2,000\times$  (Fig. 5; top right), quadrupled to  $4,000\times$  (Fig. 5; bottom left), or magnified eight times to  $8,000\times$  (Fig. 5; bottom right). While the image in Fig. 5 does not so indicate, when the image is viewed on the computer screen, individual pixels can be viewed in the  $8,000\times$  magnification (Fig. 5; bottom right). Therefore, it is possible to measure distances by counting pixels. The software assists with many other tasks such as scanning and image an finding the center of the brightest or darkest region each of which is useful in making a precision measurement.

Calibration scale dimensions were measured with the micrometer microscope stage and with the DIMMS system. The results are shown in Table 1 shown just below Fig. 5. As may be seen, the maximum error using the DIMMS is less than 2% in all cases. Also, it appears that the error tends to decrease with increasing magnification and is probably associated with being better able to determine the location of an edge of a division boundary

on the scale. It should be noted that each row in the table represents the average of more than 30 measurement for each magnification. The conclusion to draw from Table 1 is that it is very definitely possible

to measure distances of  $10\text{ }\mu\text{m}$  with high precision with the DIMMS. However, as will be demonstrated, the strain resolution of the system is controlled by the least pixel map of several items including the camera, the frame grabber board and the video monitor. The result is that strain measurement cannot be made very accurately for values less than about 0.5 % and, practically speaking, 1 % is probably more likely the lower bound that would be recommended. Obviously, by increasing the pixel map of the camera and frame grabber board to  $2\text{k} \times 2\text{k}$  or more would result in much greater strain resolution and much greater accuracy.

### **Measurement of Strain in an Adhesively Bonded Beam in Three Point Bending**

The system described above was used to measure strains in adhesively bonded three point bend specimens. As a beam loaded in three point bending is the same as two cantilevers back-to-back, the analytical solution given in an earlier section could be used to calculate stress. By measuring the relative shear deformation across the bondline using the DIMMS, the shear modulus could be determined.

Aluminum/epoxy beam specimens ( $3.86\text{ mm} \times 5.15\text{ mm} \times 35\text{ mm}$ ) were made with large bondline thicknesses ( $1.14\text{ mm}$ ) to increase the gage length and thereby increase measurement accuracy. The surfaces of the specimens were polished and small indentations were created in the aluminum immediately adjacent to the bondline. The indentations served as reference marks which could easily be located within the camera pixel map and

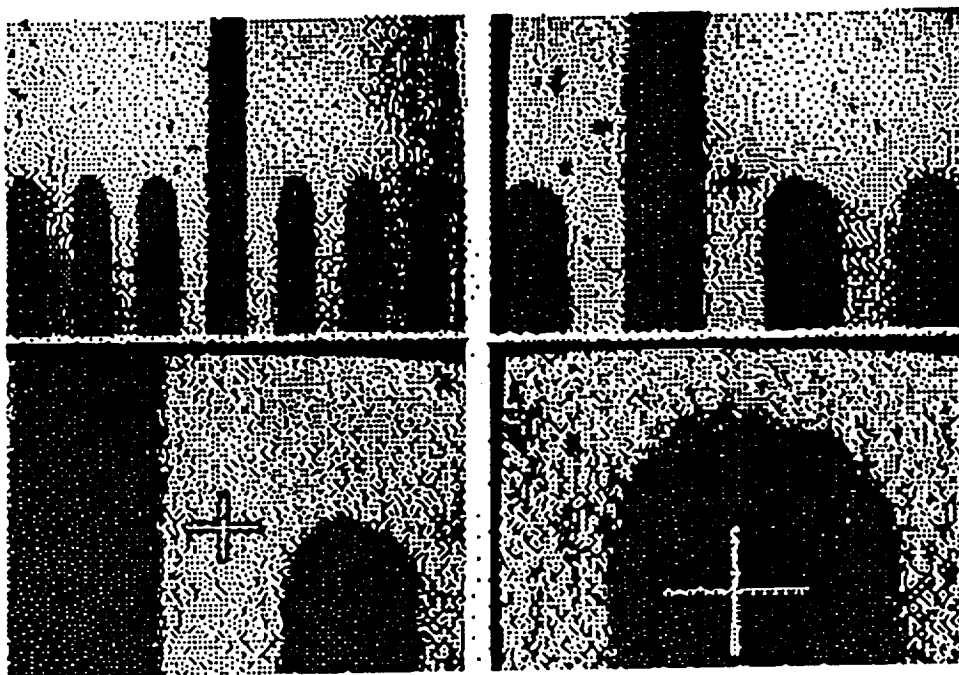


Figure 5. Digital image of calibration scale. Each small division is 10  $\mu\text{m}$ . Top left; 1,000 x. Top right; 2,000 x. Bottom left; 4,000 x. Bottom right; 8,000 x.

Table 1. Comparison of measurements of calibration scale.

Mag.	Pixels/ Micron	Actual Length ( $\mu\text{m}$ )	Measured Length			
			Microscope Stage ( $\mu\text{m}$ )	% Error	Digital Imaging ( $\mu\text{m}$ )	% Error
50x	0.351	1000.00	1000.17	0.017	1000.69	0.031
		100.00	100.13	0.130	100.36	0.357
		50.00	50.03	0.067	49.60	0.793
100x	0.709	500.00	500.10	0.020	499.83	0.035
		50.00	50.03	0.067	49.47	1.050
		20.00	19.97	0.167	20.39	1.950
200x	1.418	300.00	300.20	0.067	300.18	0.058
		50.00	50.03	0.067	49.76	0.489
		20.00	19.97	0.167	19.83	0.872
400x	2.825	150.00	150.03	0.022	149.76	0.162
		50.00	50.03	0.067	49.93	0.137
		10.00	10.00	0.000	9.97	0.300
1000x	7.02	50.00	50.00	0.000	49.98	0.045
		20.00	20.03	0.167	20.04	0.180
		10.00	10.00	0.000	9.98	0.180

thereby used to measure the relative shear displacement between adherends. As the specimen was loaded, a recording of the image being viewed by the camera was made with the VCR. Later the test was viewed frame by frame, various frames were frozen and the location of the indentations within the pixel map were used to determine the relative displacement between adherends and hence the shear strain. Figure 6 shows a photograph of images taken directly from the computer screen for different load levels. The upper left image is near the beginning of the test and the load increases from left to right and top to bottom with the bottom right frame being near the end of the test. The dark vertical regions on either side of an image are portions of the adherends (only a small portion of each adherend could be viewed even at the low magnification of 50x) and the light region between the adherends is the adhesive. That is, in Fig. 6 the beam is vertical. The dark trapezoid between the adherends is a region connecting the four indentations, two in each adherend. This region is "painted" with the software program simply to make viewing of the deformation process easier. (In the photos and on the computer screen, this region is actually green, the adherends are blue and the adhesive is white). The horizontal line has been added to give a reference line such that the change in shear strain can easily be seen. The strain in the last frame is quite large and is likely past the yield point of the aluminum.

Strain measurements were made with the DIMMS system as previously described and the results are shown in Fig. 7. In Fig. 7, the load and elongation are given on the left vertical and lower horizontal axes respectively while the strain and stress are given on the top and right axes respectively. The strain has been determined using the displacements determined with the DIMMS and the stress has been determined using equation (3). The VCR and the constant rate test frame were started at the same time. As a result, the time scale of the screw driven elongation

and the time scale of the VCR were matched such that stress and strain points could be properly located on the load elongation curve.

### **Damage Assessments of Simulated Bondline Flaws Using DMTA**

As previously indicated, the adhesive layer of an end loaded bonded cantilever beam with appropriate dimensions and adhesive/adherend moduli will be in a state of pure shear. A pure state of shear stress will also be present in the adhesive layer of a bonded fixed/fixed beam and viscoelastic adhesive shear moduli can be obtained using standard DMTA procedures. For monolithic polymer beams, it is known that the loss modulus (or  $\tan \delta$ ) is a measure of energy dissipation. For bonded metallic beams, the loss modulus (or  $\tan \delta$ ) will also be a measure of energy dissipation of the adhesive layer and/or bonding mechanisms. Should the bond (either adhesive and/or interphase) become damaged due to excessive load, fatigue, moisture or corrosion, it would seem likely that dissipation mechanisms or loss modulus and  $\tan \delta$  would change. If so the procedures outlined earlier and given in detail in references [1-7] could provide an estimate of the degree of damage and perhaps lead to quantification of the remaining life or strength. To confirm this conjecture, a series of DMTA tests were performed on beams containing simulated flaws. (Tests were also conducted on beams taken from lap specimen which had been exposed to humidity and/or corrosion for extended periods. These results are being reported elsewhere [20]).

Electro-galvanized steel (E60 EZG 60G, from Advanced Coating Technologies, Inc.) platens with dimensions of 0.29 mm x 55mm x 100mm were first wiped clean with acetone and a one-component paste epoxy adhesive (Terokal 4520-34, from Teroson, Inc.) was spread on both

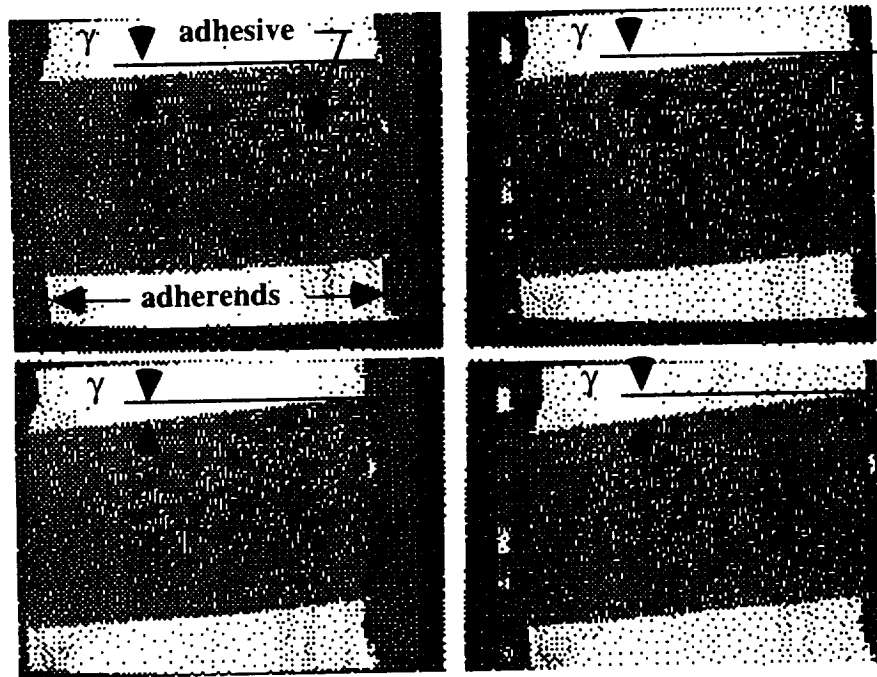


Figure 6. Images from computer screen showing the shear deformation in the adhesive. Load increases from left to right and top to bottom. (Three point bend specimen is vertical).

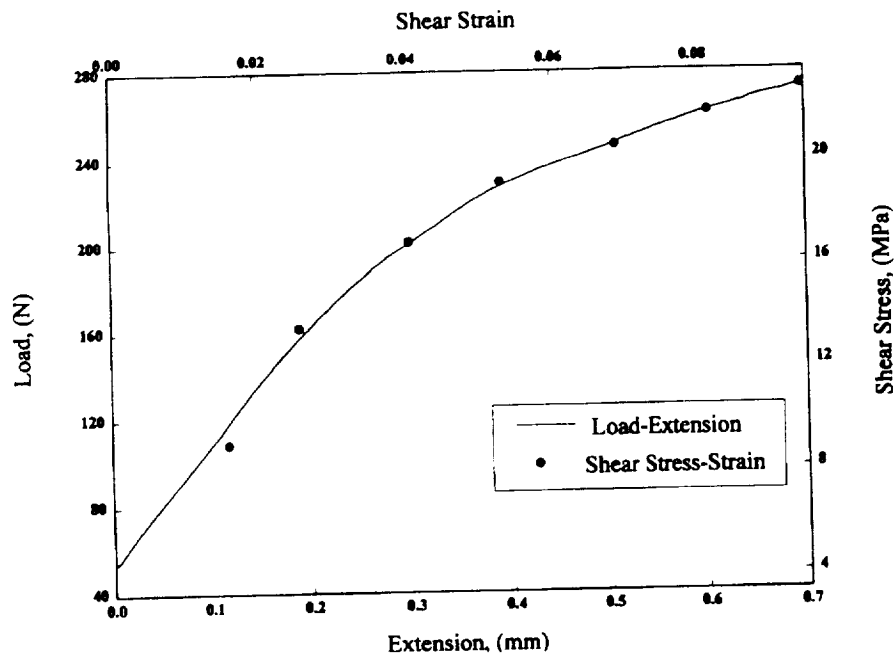


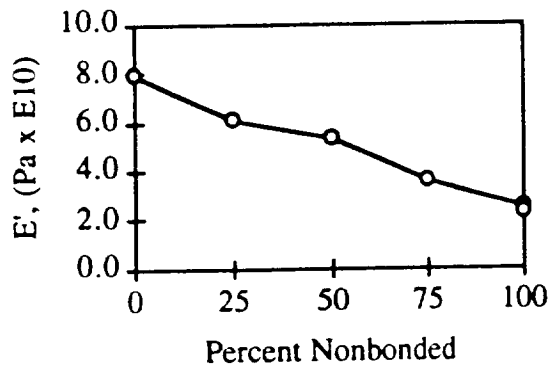
Figure 7. Shear stress strain diagram for adhesive.

mating surfaces with a spatula. The platens were pressed together so as to avoid the inclusion of air bubbles. Adhesive thicknesses were controlled using 0.35mm metal shims. The platens were clamped and the resulting sandwich was placed in a convection oven and cured for 30 minutes at 180° C. Specimens to be tested were machined from each platen. Bond lines were examined for air bubbles and for uniform thickness. Similarly, platens were made with release paper inclusions such that the resulting beams contained centrally embedded interfacial flaws of 0%, 25%, 50%, 75% and 100%. For the 100% simulated flaw, specimens were tested with a cured but unbonded epoxy layer (but no release paper) between the adherends and with a cured but un-

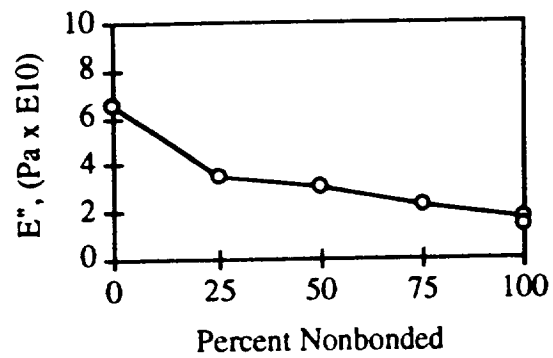
bonded epoxy layer (with release paper on each side) between the two adherends.

Specimens taken from platens with simulated flaws were tested in a DMTA (Polymer Laboratories, Amherst MA) with a standard driving unit to determine dynamic viscoelastic properties of bonded EGS beams. The geometry and loading was the same as that shown in Fig. 3 and in all cases specimen dimensions were ~ 1.8mm x 2.5mm x 32mm with a distance of 19 mm between clamps. Testing frequencies for each beam were 1.0 and 10 Hz with an end displacement (peak to peak) of 16  $\mu$ m. Temperatures were scanned from - 50° C to 200° C at a rate of 1.5° C / min.

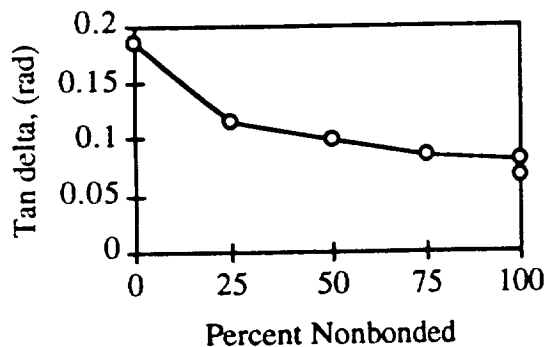
Figure 8 shows the resulting variation of storage modulus, loss modulus,  $\tan \delta$ ,



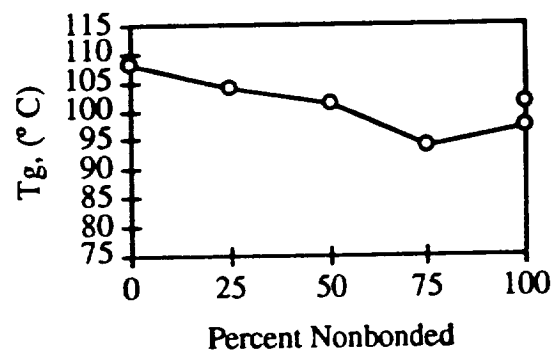
(a) E' @ 25° C



(b) E'' @ maximum  $\tan \delta$



(c) Maximum  $\tan \delta$



(d) Tg @ maximum  $\tan \delta$

Figure 8. Variation of storage modulus, loss modulus,  $\tan \delta$  and Tg with length of simulated flaw for an EGS/Epoxy beam.

and  $T_g$  for increasing length of simulated flaw (labeled Percent nonbonded) using a DMTA. Storage modulus variations were taken at 25 °C while loss modulus,  $\tan \delta$  and  $T_g$  were taken at the peak of the loss modulus curves at the temperature indicated by the  $T_g$ . As may be seen, a systematic decrease of all quantities were found as the length of the simulated flaw (non bonded length) increased. Using the analysis of Dickie, et. al. [18, 19], it would be possible to unambiguously assign a discrete value to the loss in energy due to the simulated flaw. However, as mentioned in the earlier section, their analysis needs to be changed to incorporate the new approach suggested by the static analysis. This is in progress and will be reported subsequently. While the data in Fig. 8 does indicated that the DMTA can give an indication of simulated damage, it is now necessary to determine if the procedure can be used to discriminated differences in real damage due to fatigue, moisture or corrosion. Brinson, Dickie and DeBolt have shown that similar procedures can be used to assess the damage in specimens subjected to prolonged exposure to both humidity and corrosion [20]. These data are being reported elsewhere. Fatigue tests have not yet been attempted but are in the planning stage.

### Measurement of Strain in a Composite Beam in Three Point Bending

As indicated in the introduction, a design approach being considered for the HSCT is to be able to predict the change in a composite structure due to aging, memory, environmental and other effects as well as their combination by knowing how the fiber, resin and interface constituents change due to the same effects. Earlier studies have suggested the resin as cured in the composite does not exhibit the same behavior as the resin when cured alone.

As a result, an exploratory study was undertaken to determine if the DIMMS approach described earlier could be used to measure the properties of the resin in a composite in resin rich regions between the plies and possibly between the fibers.

Three point bend [90]<sub>16</sub> carbon/epoxy (IM7/5260) composite beams with the dimensions of 2.31mm x 4.5mm x 40mm were polished and tested under constant head rate conditions. A digitized photomicrograph of the edge of a composite beam is shown in Fig. 9. Individual fiber ends are clearly visible as well as the resin rich region between plies near the outer tensile surface. Two fibers at the edge of the resin rich region were selected as targets and used to estimate the tensile deformation as the test progressed. Strains were determined from these deformations and stress was determined using elementary beam theory. From these data the transverse modulus of the composite was determined to be approximately  $1.6 \times 10^6$  and were nearly the same as results determined in tensile tests by Dr. M. Tuttle of the University of Washington who supplied us with the IM7/5260 material [21]. Modulus values did vary during the test and, in fact seem to increase for larger deformations. Thus it is clear that serious deficiencies with our equipment exist at present and that the resolution of the DIMMS system as presently constituted is operating at the threshold of accuracy needed for serious investigation of composite materials. However, it is believed that with modifications to the load frame and with a high resolution camera, frame grabber board, etc. containing at least a 2k x 2k pixel map, the appropriate accuracy of deformation can be achieved to reliably measure the properties of the resin as cured in a composite.

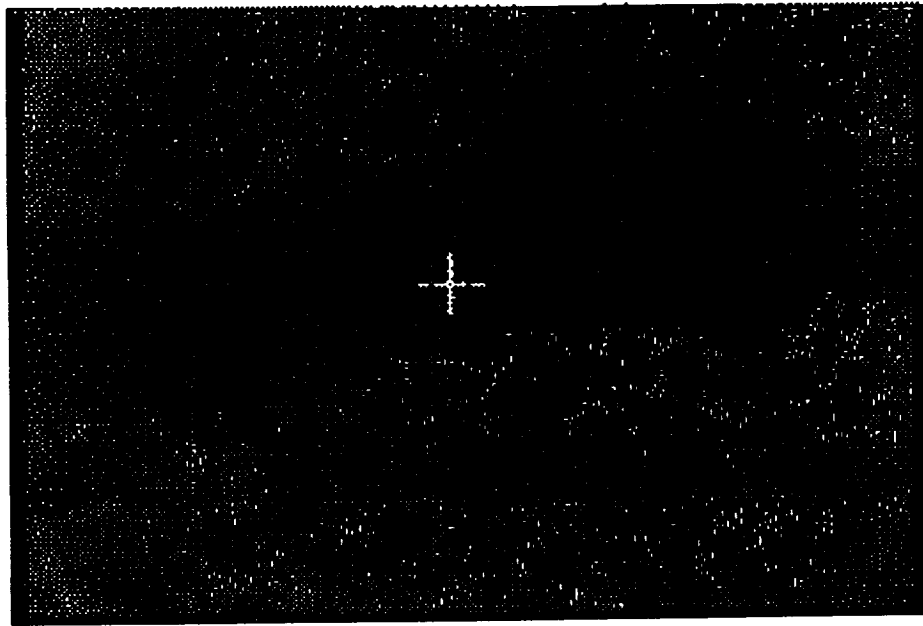


Figure 9. Digital image of photomicrograph of a unidirectional  $[90]_{16}$  carbon/epoxy (IM7/5260) composite at 400 x.

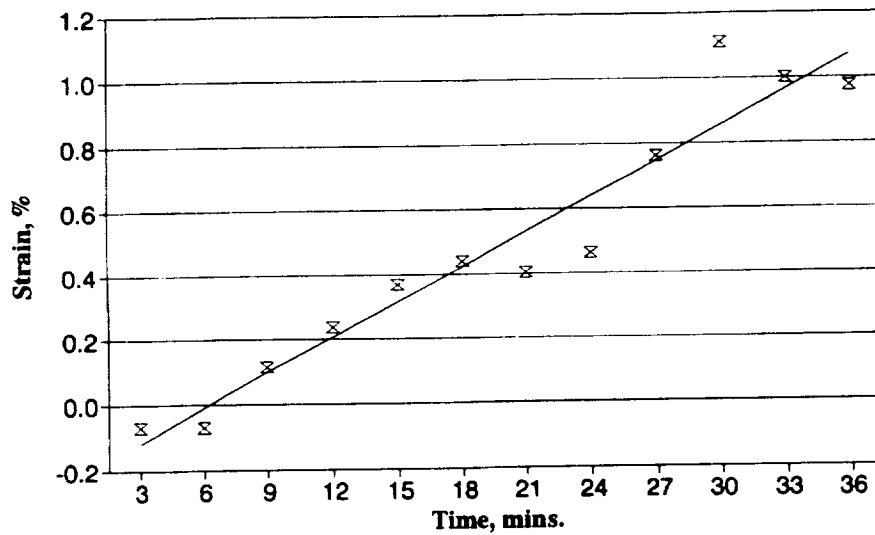


Figure 10. Measured strain in resin rich region of a composite beam in three point bending under constant head rate conditions. Symbols are measurements and the solid line is the approximate "best fit".

## Summary and Conclusions

A new digital imaging micro-measurement procedure has been described. The procedure has been used to determine strains in a bonded joint and within the resin rich region of a composite. It has been shown that this optical DIMMS procedure can be used to measure distances as small as 10  $\mu\text{m}$  with an error no greater than 2%. The smallest strains that can be measured with the present system is about 1% but with higher resolution cameras with a pixel map of 2k x 2k or better, it should be possible to measure strains as small as 0.2%. The transverse modulus of a composite so determined was found to be approximately the same as that determined by traditional tensile testing procedures.

A double cantilever bonded beam specimen has been described that contains a pure state of shear stress in the bond line and a simple strength of materials analysis has been reviewed. This specimen should prove useful for routine measurement of the pure shear properties of adhesives and in combination with the DIMMS approach should allow the determination of strains with the bondline. With more sophisticated instrumentation, it should be possible to determine strain distributions across the bondline and perhaps, ultimately be used to measure strains near or within the interphase regions.

It should be pointed out that the micro-measurement procedures outlined herein are only in their infancy. Higher resolution cameras are already available and when used in conjunction with scanning electron microscopes, it is now possible to make measurements in sub-micron domains [22,23]. Figure 11 is a chart indicating the size regions within which several current methods of strain measurement procedures can be used. Also, the size of a typical interphase region for an adhesive bond is given along with the resolution provided by several microscopes or magnification devices which

have the potential of being used for micron and sub-micron examination of materials. As will be noted, the most popular techniques of extensometers, electrical strain gages, photoelasticity etc. are relatively coarse measurements and do not give property values over the same small size regions within which analytical calculations can be made. That is, with the finite element method, it is possible to determine stress and strain values within infinitesimal regions adjacent to crack tips, interfaces, etc. On the other hand, currently only average strains over relatively large regions can be found for comparison purposes. Thus, with the development of better micro-measurement procedures, as is clearly possible from an examination of Fig. 11., it will be possible to better understand the behavior of materials at scales which match our computational abilities.

The value of micro-measurement methods is clear as they may ultimately allow the measurement of strains in domains that match the same scale now possible with our analytical procedures. A companion benefit, and perhaps of equal or greater importance, will be the ability to observe deformation mechanisms at the same time they are being measured. Therefore, a better understanding of material behavior should result.

An approach to assess simulated damage in an adhesive joint using a DMTA has been presented and it is suggested that it may lead to a simple procedure to assess hidden states of damage in adhesive joints (or perhaps composite materials also) due to fatigue, moisture, corrosion or other parameters. It should be noted, of course, that a DIMMS approach could be used in conjunction with a DMTA using strobe lighting and it might be possible to measure strains within the bondline of an adhesive as damage is accumulating.

This author suggests that new digital imaging measurement techniques will eventually become routine tools for the



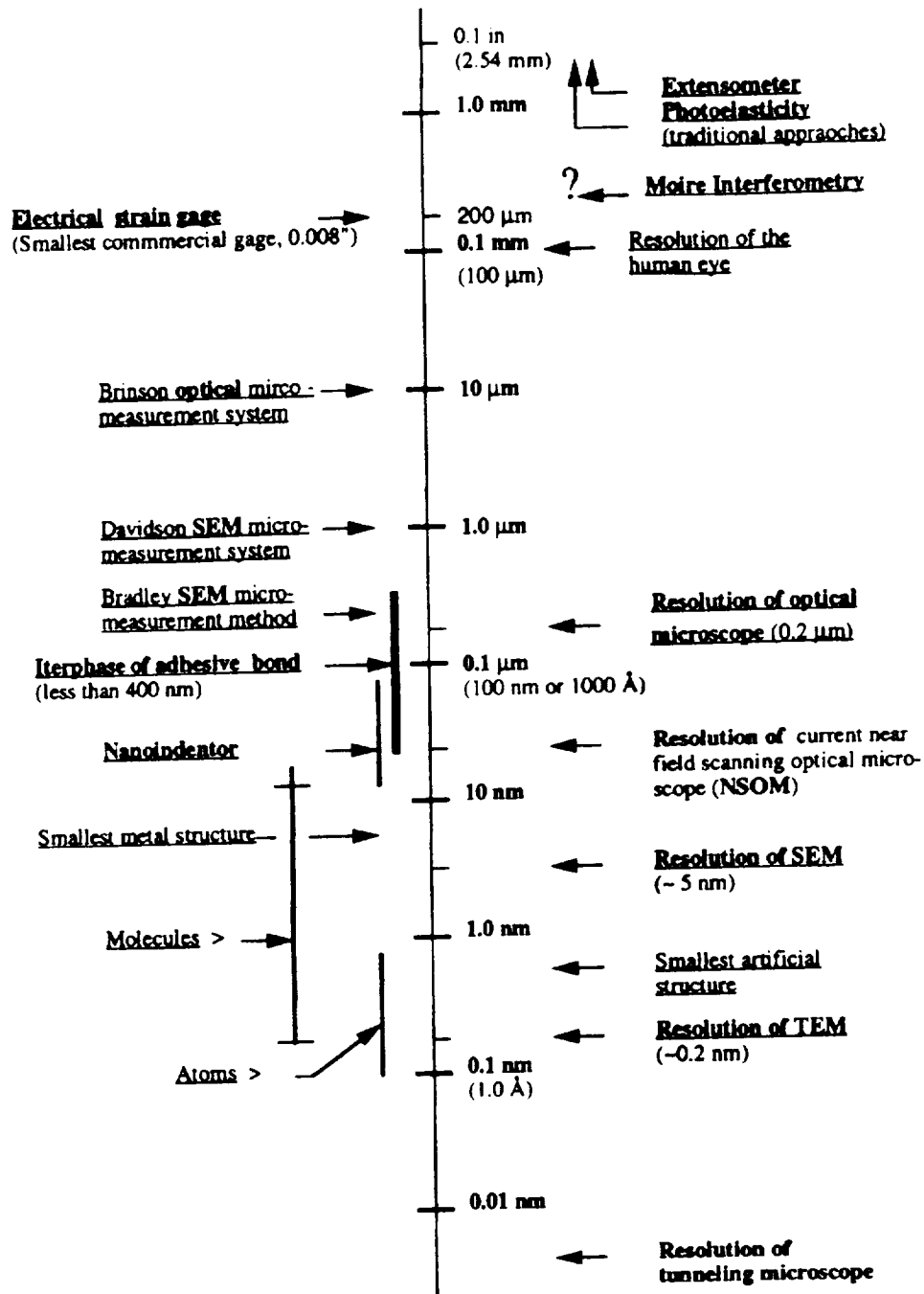


Figure 11. Scale comparing the minimum size region within which various strain measuring techniques can be used. Size of adhesive interphase is also shown and the resolution of various new microscopes with the potential of being used in micro-measurement systems.

person engaged in experimental mechanics. It is hoped that the present effort may in a small way lead to the further development of such procedures.

### Acknowledgments

The author is pleased to acknowledge the long time support of NASA Ames Research Center (Dr. H. Nelson, monitor) and the Naval Research Laboratory (Dr. L. Peebles, monitor). The present support of the Boeing Commercial Airplane Co. (Dr. R. Khanna, monitor) is also greatly appreciated. A special thanks is due to the Ford Motor Co. (Dr. R. Dickie, sponsor) and to the U. of Poitiers (Dr. A. Lagarde, sponsor) for providing an unusual opportunity to spend several months in concentrated effort examining the various potential aspects of the bonded DCB specimen. Finally, appreciation is extended to UTSA Research Assistants E. Brock and G. MacKay for their excellent experimental and computer skills in the development and operation of our Micro-Measurements and Micro-Mechanics Laboratory as well as the other laboratory assistants who have helped with this endeavor.

### References

1. Brinson, H. F., Morris, D. H., and Yeow, Y. T., "A New Experimental Method for the Accelerated Characterization and Prediction of the Failure of Polymer-Based Composite Laminates," *Proceedings 6th International Conference for Experimental Stress Analysis*, Munich, Munich, 1978, pp. 395.
2. Morris, D. H., Yeow, Y. T., and Brinson, H. F., "The Viscoelastic Behavior of the Principal Compliance Matrix of a Unidirectional Graphite-Epoxy Composite," *Polymer Composites*, Sept. 1980, Vol. 1, No. 1, pp. 32.
3. Cartner, J. S., Griffith, W. I., and Brinson, H. F., "The Viscoelastic Behavior of Composite Materials for Automotive Applications," *Composite Materials in the Automotive Industry*, ASME, NY, 1978, pp. 159.
4. Dillard, D. A., Morris, D. H., and Brinson, H. F., "Predicting Viscoelastic Response and Delayed Failures in General Laminated Composites," *ASTM STP 787, Composite Materials: Testing and Design (6th Conference)*, Dec. 1982, pp. 357.
5. Tougui, A., Gamby, D., Lagarde, A., and Brinson, H. F., "Nonlinear Photo-viscoelasticity: Theory and Measurement," *Experimental Mechanics*, Sept. 1983, pp. 314.
6. Brinson, H. F., Cardon, A. H., and Hiel, C. C., "Comportement Visco-elastique Non-Lineaire Des Composite A Matrice Polymerique," *JNC 4*, Sept. 10-11, 1984, Paris.
7. Tuttle, M. E. and Brinson, H. F., "Prediction of Long Term Creep Compliance of General Composite Laminates," *Proceedings of the 1985 SEM Spring Conference on Experimental Mechanics*, SEM, CT, 1985, pp. 764; *Experimental Mechanics*, March 1986, pp. 89.
8. Lefebvre, D. R., Ward, T. C., Dillard, D. A., and Brinson, H. F., "A Non-linear Constitutive Behavior for Diffusion in polymers," *J. of Adhesion*, Vol. 27, 1989, pp. 19.
9. Gramoll, K. C., Dillard, D. A., Brinson, H. F., "Thermoviscoelastic Characterization and the Prediction of Kevlar/Epoxy Composite Laminates, Composite Materials: Testing and Design (Ninth Volume), ASTM STP 1059, S. P. Garbo, Ed., ASTM, Phil., 1990, pp. 477.
10. Brinson, H. F., "A Nonlinear Viscoelastic Approach to the Durability Predictions for Polymer Based Composite Structures", *Durability of Polymer Based Composite Systems for Structural Applications*, (A. H. Cardon

- and G. Verchery, Ed.'s.), Elsevier, NY, 1991, p.46.
11. Roy, S., Reddy, J. N., and Brinson, H. F., "Geometries and Viscoelastic Non-linear Analysis of Adhesive Joints, *Mechanical Behavior of Adhesive Joints* (A. H. Cardon and G. Verchery, Ed.'s.), Euromech Colloquium 227, August 1987.
  12. Brinson, H. F., Renieri, M. P., and Herakovich, C. T., "Rate and Time Dependent Failure of Structural Adhesives," *Fracture Mechanics of Composites*, STP 617, American Society for Testing and Materials (ASTM), Phil., 1975, pp. 177.
  13. Brinson, H. F., Wightman, J. P., Dillard, D. A., Lefebvre, D., and Filbey, J., "Test Specimen Geometry's for Evaluating Adhesive Durability," *Proceedings of the 19th International SAMPE Technical Conference*, Vol. 19, Oct. 1987, pp. 152.
  14. Moussiaux, E., Cardon, A. H. and Brinson, H. F., "Bending of a Bonded Beam as a Test Method for Adhesive Properties," *Mechanical Behavior of Adhesive Joints* (A. H. Cardon and G. Verchery, Ed.'s.), Euromech Colloquium 227, Pluralis, Paris, p. 1, August 1987.
  15. Moussiaux, E., "Bending of a Bonded Beam as a Test Method for Adhesive Properties," M. S. Thesis Virginia Tech, June 1987. (Also, Moussiaux, E., Cardon, A. H., and Brinson, H. F., VT Report, VPI-E-87-9 and/or CAS/ESM-87-2, June 1987).
  16. Fior, Valerie, "A Beam Test for Adhesives," M. S. Thesis, Virginia Tech, June, 1988. (Also, VT Report, VPI-E-88/21/CAS/ESM 88-8, July 1988).
  17. Brinson, H. F., Brock, E. A., and MacKay, G. A., "Adhesive Pure Shear Properties via a Bonded Double Cantilever Beam Specimen", UTSA Micro-Measurement and Micro-Mechanics Laboratory Report, MMMLR-1, UTSA, July 1994. (Also, Society for Engineering Science, College Station, Oct. 1994).
  18. Li, C., Dickie, R. A., and Moreman, K. N., "Dynamic Mechanical Response of Adhesively Bonded Beams: Effect of Environmental Exposure and Inter-facial Properties", *Polymer Engineering and Science*, Feb. 1990, Vol. 30, No. 4, p. 249.
  19. Moreman, K. N., Li, C., Zhang, F., Dickie, R. A., "Determination of the Complex Shear Modulus of Structural Adhesives Using a doubly Clamped Sandwich Beam", *Experimental Mechanics*, June 1992, p. 124.
  20. Brinson, H. F., Dickie, R. A. and DeBolt, M. A., "Measurement of Adhesive Bond Properties Including Damage by Dynamic Mechanical Thermal Analysis of a Beam Specimen", (in review, June 1994).
  21. Tuttle, M. A., Private Communication, March 1994.
  22. Williams, D. R., Davidson, D., L and Lankford, J. Fatigue-crack-tip Plastic Strains by the Stereoimaging Technique, *Experimental Mechanics*, Vol. 20, No. 4, April 1980, pp. 134.
  23. Carlito, C., Bradley, W.O. and Brinson, H. F., Final NSF Report, August 1992.